Published in final edited form as:
Int J Biochem Cell Biol. 2009 May ; 41(5): 1216–1227. doi:10.1016/j.biocel.2008.11.001.

A novel adhesion molecule in human breast cancer cells: Voltage-gated Na^+ channel β1 subunit

Athina-Myrto Chioni[1,*], **William J. Brackenbury**[2,*], **Jeffrey D. Calhoun**[2], **Lori L. Isom**[2], and **Mustafa B. A. Djamgoz**[1]

1*Neuroscience Solutions to Cancer Research Group, Division of Cell and Molecular Biology, Sir Alexander Fleming Building, Imperial College London, South Kensington Campus, London, SW7 2AZ, UK*

2*Department of Pharmacology, University of Michigan Medical School, Ann Arbor, MI 48109-0632, USA*

Abstract

Voltage-gated Na^+ channels (VGSCs), predominantly the 'neonatal' splice form of $Na_v1.5$ ($nNa_v1.5$), are upregulated in metastatic breast cancer (BCa) and potentiate metastatic cell behaviours. VGSCs comprise one pore-forming α subunit and one or more β subunits. The latter modulate VGSC expression and gating, and can function as cell adhesion molecules of the immunoglobulin superfamily. The aims of this study were (1) to determine which β subunits were expressed in weakly metastatic MCF-7 and strongly metastatic MDA-MB-231 human BCa cells, and (2) to investigate the possible role of β subunits in adhesion and migration. In both cell lines, the β subunit mRNA expression profile was *SCN1B* (encoding β1) ≫ *SCN4B* (encoding β4) > *SCN2B* (encoding β2); *SCN3B* (encoding β3) was not detected. MCF-7 cells had much higher levels of all β subunit mRNAs than MDA-MB-231 cells, and β1 mRNA was the most abundant. Similarly, β1 protein was strongly expressed in MCF-7 and barely detectable in MDA-MB-231 cells. In MCF-7 cells transfected with siRNA targeting β1, adhesion was reduced by 35 %, while migration was increased by 121 %. The increase in migration was reversed by tetrodotoxin (TTX). In addition, levels of $nNa_v1.5$ mRNA and protein were increased following β1 down-regulation. Stable expression of β1 in MDA-MB-231 cells increased functional VGSC activity, process length and adhesion, and reduced lateral motility and proliferation. We conclude that β1 is a novel cell adhesion molecule in BCa cells and can control VGSC ($nNa_v1.5$) expression and, concomitantly, cellular migration.

Keywords

Adhesion; breast cancer; metastasis; migration; voltage-gated Na^+ channel

1. Introduction

Voltage gated Na^+ channels (VGSCs) are classically responsible for action potential generation and conduction in excitable cells (Catterall, 2000). VGSCs contain one pore-forming α subunit

Correspondence to: Professor M. B. A. Djamgoz, Neuroscience Solutions to Cancer Research Group, Division of Cell and Molecular Biology, Sir Alexander Fleming Building, Imperial College London, London SW7 2AZ, UK, Tel: (0) 207 594 5370, Fax: (0) 207 584 2056, Email: E-mail: m.djamgoz@imperial.ac.uk.
*These authors contributed equally.

and one or more β subunits (Catterall, 1992). VGSCs are also widely expressed in cells from a range of human cancers, including breast cancer (BCa) (Fraser et al., 2005, Roger et al., 2003), prostate cancer (PCa) (Laniado et al., 1997), lymphoma (Fraser et al., 2004), lung cancer (Onganer and Djamgoz, 2005, Roger et al., 2007), mesothelioma (Fulgenzi et al., 2006), neuroblastoma (Ou et al., 2005), melanoma (Allen et al., 1997) and cervical cancer (Diaz et al., 2007). In addition, VGSCs are upregulated in line with metastasis in BCa, PCa, and small-cell lung cancer (SCLC) in vivo (Onganer et al., 2005, Fraser et al., 2005, Diss et al., 2005).

In human and rodent cell models of BCa, PCa and lung cancer, the specific VGSC blocker tetrodotoxin (TTX) suppresses a variety of in vitro metastatic cell behaviours including invasion (Grimes et al., 1995, Bennett et al., 2004, Laniado et al., 1997, Roger et al., 2003), migration (Brackenbury and Djamgoz, 2006), galvanotaxis (Djamgoz et al., 2001), morphological development and process extension (Fraser et al., 1999), endocytic membrane activity (Onganer and Djamgoz, 2005), lateral motility (Fraser et al., 2003), adhesion (Palmer et al., 2008) and gene expression (Brackenbury and Djamgoz, 2006). Strongly metastatic MDA-MB-231 human BCa cells express a TTX-resistant (IC_{50} in μM range) VGSC current that is absent in weakly metastatic MCF-7 cells (Fraser et al., 2005, Roger et al., 2003). In MDA-MB-231 cells, the predominant α subunit ($Na_v1.5$; gene: *SCN5A*) is expressed primarily in its 'neonatal' D1:S3 5'-splice form ($nNa_v1.5$) (Chioni et al., 2005, Fraser et al., 2005). $nNa_v1.5$ is primarily responsible for the VGSC-dependent enhancement of migration and invasion of MDA-MB-231 cells (Brackenbury et al., 2007). However, the possible functional involvement of β subunits in potentiation of metastatic cell behaviours is not yet known.

So far, four VGSC β subunits (β1-β4; genes: *SCN1B-SCN4B*) have been identified. β1 and β3 are non-covalently associated with the α subunit (Morgan et al., 2000, Isom et al., 1992), whereas β2 and β4 are disulphide linked (Isom et al., 1995, Yu et al., 2003). VGSC β subunits are multifunctional molecules (Brackenbury and Isom, 2008). These are unique among ion channel auxiliary subunits in that they are homologous to the immunoglobulin superfamily of cell adhesion molecules (CAMs) (Isom, 2001, Isom et al., 1994). β subunits also direct α subunit insertion into the plasma membrane and permit interaction of the channel with other signalling proteins. For example, β1 and β2 interact with the extracellular matrix proteins tenascin-C and tenascin-R, influencing neuronal migration (Xiao et al., 1999, Srinivasan et al., 1998). In addition, β1 and β2 participate in homophilic cell adhesion, resulting in cellular aggregation and ankyrin recruitment (Malhotra et al., 2002, Malhotra et al., 2000). Furthermore, β1 interacts heterophilically with N-cadherin, contactin, neurofascin-155, neurofascin-186, NrCAM and β2 (Malhotra et al., 2004, Kazarinova-Noyes et al., 2001). β1 promotes process extension, migration and pathfinding in neurones (Brackenbury et al., 2008a, Davis et al., 2004). β1 can also influence intracellular mechanisms, e.g. a site within the cytoplasmic domain of β1 interacts with receptor tyrosine phosphatase β (Ratcliffe et al., 2000). At least some of these functional roles may be independent of α subunits; in fact, it has been suggested that independent β subunit functioning may be equally important (Malhotra et al., 2002, Fein et al., 2008). β subunits may have direct involvement in pathophysiologies, e.g. cardiac arrhythmia, epilepsy and pain (reviewed in Brackenbury and Isom, 2008) and indirect involvement, via interacting partners, e.g. contactin, as in metastasis (Su et al., 2006). A recent study on human prostate cancer found (i) that the β subunit mRNA level in vitro was positively correlated with metastatic potential and (ii) that *SCN1B* was most abundant (Diss et al., 2007). β subunit expression in human BCa has not previously been studied.

The main aims of the present study were twofold: (1) to investigate β subunit expression in two human BCa cell lines of contrasting metastatic potential: MCF-7 (non/weakly metastatic) and MDA-MB-231 (strongly metastatic) in a comparative approach; and (2) to explore the involvement of the β subunit(s), mainly β1, in cellular adhesion and migration.

2. Materials and methods

2.1 Cell culture

MDA-MB-231 and MCF-7 cells were cultured in Dulbecco's modified Eagle's medium supplemented with 5-10 % foetal bovine serum (FBS) and 4 mM L-glutamine, as described previously (Fraser et al., 2005).

2.2 Real-time PCR

RNA extraction, cDNA synthesis and real-time PCR were performed as described previously (Brackenbury et al., 2007). Primers for Cytb5R and $nNa_v1.5$ were as described previously (Diss et al., 2001, Brackenbury et al., 2007). The following primer pairs and annealing temperatures were also used:

1. *SCN1B*: 5'-AGAAGGGCACTGAGGAGTTT-3'and 5'-GCAGCGATCTTCTTGTAGCA-3' (60 °C).
2. *SCN2B*: 5'-GAGATGTTCCTCCAGTTCCG-3' and 5'-TGACCACCATCAGCACCAAG-3' (62 °C).
3. *SCN3B*: 5'-CTGGCTTCTCTCGTGCTTAT-3' and 5'-TCAAACTCCCGGGACACATT-3' (60 °C).
4. *SCN4B*: 5'-TAACCCTGTCGCTGGAGGTG-3' and 5'-TGAGGATGAGGAGCCCGATG-3' (60 °C).

Threshold amplification cycles were determined using the Opticon Monitor 2 software (MJ Research, Waltham, MA) and analysed by the $2^{-\Delta\Delta Ct}$ method (Livak and Schmittgen, 2001).

2.3 RNA interference

RNA interference was performed with a pool of siRNAs (Genome smart pool for human *SCN1B* NM_001037; Dharmacon, Lafayettte, CO), as described previously (Brackenbury et al., 2007). mRNA and protein levels were measured 4-12 days after transfection, and compared with two controls:

1. 'Mock'. Transfection without siRNA.
2. 'siControl'. Transfection with siControl Non-Targeting siRNA pool (Dharmacon).

Transfection efficiency was assessed independently using a positive control siRNA targeting Lamin A/C (Dharmacon), which significantly reduced the lamin A/C protein level by ≥ 70 % after 4 days, compared to siControl non-targeting siRNA.

2.4 Creation of a stable MDA-MB-231 line expressing β1

Cells (50 % confluent) were transfected overnight with cDNA (2 μg) using Fugene6 reagent (Roche, Nutley, NJ, USA). cDNA encoding eGFP was subcloned from pEGFPN1 into $pcDNA3.1^+$ (Invitrogen). β1-GFP was generated by inserting β1 cDNA lacking the stop codon into pEGFPN1 to create a C-terminal fusion protein. The β1-eGFP cDNA was then subcloned into $pcDNA3.1/Hygro^+$. eGFP-transfected cells were selected with 400 μg/ml geneticin. One clone was derived and maintained in 200 μg/ml geneticin. β1-eGFP-transfected cells were selected with 200 μg/ml hygromycin B. One clone was derived and maintained in 100 μg/ml hygromycin B.

2.5 Western blotting

Total cell lysate preparation, cell membrane preparation, SDS polyacrylamide gel electrophoresis, transfer to nitrocellulose and chemiluminescent detection were performed as

described previously (Lopez-Santiago et al., 2006, McEwen et al., 2004, Laniado et al., 1997, Chioni et al., 2005, Fraser et al., 2005). The following primary antibodies were used:

1. Pan-Na^+ channel α subunit antibody (1 μg/ml; Millipore, Watford, UK);
2. NESO-pAb antibody (1 μl/ml) (Chioni et al., 2005);
3. Anti-$\beta1_{ex}$ antibody (1:500) (Malhotra et al., 2002);
4. Anti-actin antibody (1:700; Sigma, Dorset, UK);
5. Anti-actinin antibody (1 μl/ml; Sigma);
6. Anti-GFP A-11121 (1:1000; Invitrogen).

Densitometric analysis was performed using the Image-Pro Plus software (Media Cybernetics, Bethesda, MD, USA). Signal density was normalised to anti-actinin or anti-actin antibody as a loading control/reference, for at least three separate experiments. For each antibody, linearity of signal intensity with respect to increasing protein loading in the range 20-80 μg was ensured using a standard dilution of MDA-MB-231 cell extract.

2.6 Immunocytochemistry and confocal microscopy and image analysis

Cells (2×10^4) grown on poly-L-lysine-coated glass coverslips were fixed in paraformaldehyde (2 %) and labelled with fluorescein isothiocyanate (FITC)-conjugated concanavalin A (conA; Sigma) as plasma membrane marker (Brackenbury and Djamgoz, 2006). Nonspecific binding sites were blocked with 5 % FBS prior to incubation with NESO-pAb. The secondary antibody was Alexa567-conjugated goat anti-rabbit IgG (Dako). Cells were mounted in Vectashield (Vector Laboratories, Peterborough, UK). Fluorescence was detected using a Leica (Wetzlar, Germany) DM IRBE microscope with TCS-NT confocal laser scanner. GFP was detected using an Olympus (Tokyo, Japan) Fluoview 500 confocal laser-scanning microscope. Densitometric analysis was performed as described previously (Brackenbury and Djamgoz, 2006). Measurements were taken from at least 50 cells per condition, for three repeat treatments.

2.7 Electrophysiology

Whole-cell recording of Na^+ currents from cells grown on glass coverslips was performed as decribed previously, with some modifications (Brackenbury et al., 2007). Patch pipettes (TW150F-3, WPI, Sarasota, FL, USA) were pulled using a Model P-97 puller (Sutter Instruments, Novato, CA, USA) and fire-polished to give resistances of 2-3 MΩ when filled with internal solution. Voltage-clamp recordings were performed using a Multiclamp 700B amplifier (Molecular Devices, Union City, CA, USA) compensating for series resistance by 60 %. Currents were digitized using a Digidata 1320 interface (Molecular Devices), low-pass filtered at 10 kHz, sampled at 50 kHz and analyzed using pClamp 9.2 software (Molecular Devices). Linear components of leak were subtracted using a standard P/6 protocol (Armstrong and Bezanilla, 1977). Data manipulation and curve fitting were performed as described previously (Ding and Djamgoz, 2004).

2.8 In vitro assays of metastatic cell behaviour

Morphometric analysis—Transfected cells were viewed under a Zeiss Axioplan fluorescent microscope at The University of Michigan Microscopy and Image Analysis Laboratory. Images captured at 40X were exported into the NIH ImageJ software for analysis. The following measurements were taken for both monopolar and bipolar cells, as described previously (Fraser et al., 1999):

1. Process length;
2. Process thickness;

3. Cell body diameter. Measurements were recorded from 40 cells from each class, for each cell line.

Single-cell adhesion—Measurements were performed on cells 48 h after plating into 35 mm dishes at a density of 2.5×10^4 cells/ml, using the single-cell adhesion measuring apparatus (SCAMA), as described previously (Palmer et al., 2008). The peak detachment negative pressure (DNP), measured digitally for each cell, was converted to kPa.

Cell-cell adhesion—The cell-cell adhesion assay was performed as described previously, with some modifications (Wong and Filbin, 1996). Suspensions of single cells (2×10^6 cells/ml) were allowed to aggregate at 37 °C with gentle rocking (25 rpm). The particle number of aliquots was determined with a Coulter counter (Z_{BI}; Beckman Coulter, Fullerton, CA, USA) every 30 min for 2 h. Duplicate samples were counted three times, for three repeat experiments.

Proliferation—Cells (1×10^4 cells/ml) were seeded in triplicate wells of a 12-well plate for 24 h. The number of cells per well after 24 h was determined using the thiazolyl blue tetrazolium bromide (MTT) assay, as described previously (Grimes et al., 1995). Results were compiled as the mean of three repeats.

Transwell migration—Cells (2×10^5 cells/ml) were plated onto 12 μm-pore Transwell migration filters in 12-well plates (Corning, NY, USA). siRNA-treated and/or control cells were incubated with or without TTX (10 μM, applied once at the beginning of the assay), in a 1-10 % chemotactic FBS gradient overnight (12 h). The number of cells migrating was determined using the MTT method (Grimes et al., 1995). Results were compiled as the mean of ≥ four repeats.

Lateral motility—Wound-heal assays were performed as described previously (Fraser et al., 2003). Measurements of wound width (15 per wound) were made at wound formation (W_0) and 24 h later (W_t). The motility index (MI) was calculated as $MI = 1 - (W_t/W_0)$. Means were compiled from three repeat experiments.

2.9 Data analysis

All quantitative data are presented as means ± standard errors, unless stated otherwise. Statistical significance was determined with Student's t test, Mann-Whitney rank sum test, one-way analysis of variance (ANOVA) followed by Newman-Keuls test, or two-way ANOVA, as appropriate. Results were considered significant at $P < 0.05$ (*).

3. Results

We evaluated the expression of VGSC β subunits in weakly metastatic MCF-7 and strongly metastatic MDA-MB-231 cells in a comparative approach. β1 was then downregulated in MCF-7 cells, and stably expressed in MDA-MB-231 cells in order to elucidate its functional involvement in the cells' adhesion and migration.

3.1 Expression of VGSC α and β subunits in human BCa cell lines

Both MCF-7 and MDA-MB-231 cell lines expressed *SCN1B* (encoding β1), *SCN2B* (encoding β2) and *SCN4B* (encoding β4) mRNAs; *SCN3B* mRNA (encoding β3) was not detected in either line but could be detected in human prostate cancer PC-3M cells (Figure 1A). Two products were amplified using the *SCN4B* primers: the full-length product (459 nt), and a shorter form (310 nt; Figure 1A). Real-time PCR revealed that MCF-7 cells had 40-50 fold higher levels of all β subunit mRNAs than MDA-MB-231 cells (Table 1A; Figure 1B). In both cell lines, *SCN1B* was expressed at the highest level of any β subunit (Figure 1B). The relative

levels of mRNA in both cell lines were *SCN1B* ≫ *SCN4B* > *SCN2B* (Table 1B). Western blot analysis using anti-$\beta1_{ex}$ antibody confirmed that β1 polypeptides were highly expressed in MCF-7 and barely detectable in MDA-MB-231 cells (Figure 1C).

The mRNA level of $nNa_v1.5$, the predominant α subunit in MDA-MB-231 cells (Fraser et al., 2005), was ~4200-fold higher than in MCF-7 cells ($P < 0.05$, $n = 4$; Figure 2A). Both the total α subunit and $nNa_v1.5$ protein levels were ~4-fold higher in MDA-MB-231 than MCF-7 cells ($P < 0.01$, $n = 6$; Figure 2B).

In conclusion, β1, the most highly expressed VGSC β subunit in both MDA-MB-231 and MCF-7 cells, was significantly more abundant in the latter, non/weakly metastatic line, especially at protein level.

3.2 Silencing of β1 expression in weakly metastatic MCF-7 cells by RNAi

Cells were transfected with a pool of siRNAs targeting *SCN1B*. In siRNA-treated cells, the *SCN1B* mRNA level was reduced by 76 % after 4 days ($P < 0.01$, $n = 3$; Figure 3A, B). β1 protein was reduced by 18 % after 5 days and 40 % after 8 days ($P < 0.05$ / $n = 6$ and $P < 0.05$ / $n = 8$, respectively; Figure 3C, D). In contrast, after 4 days, mRNA levels of *SCN2B* and *SCN4B* were unaffected ($P = 0.71$ and $P = 0.97$, respectively; $n = 3$; Figure 3B).

Five days after transfection with siRNA targeting *SCN1B*, the $nNa_v1.5$ mRNA level increased by 280 % ($P < 0.05$, $n = 3$; Figure 3B). However, there was no change in either the total VGSC α subunit or $nNa_v1.5$ protein levels ($P = 0.93$ and $P = 0.42$, respectively; $n = 4$; Figure 4A, B). In contrast, 8 days after transfection, when the β1 protein level was lowest, both the total VGSC α subunit and $nNa_v1.5$ protein levels were increased by 256 % and 147 %, respectively ($P < 0.05$, $n \geq 3$; Figure 4A, B). Furthermore, 12 days post-transfection, when *SCN1B* mRNA had returned to normal, total VGSC α subunit and $nNa_v1.5$ protein levels remained elevated by 99 % and 117 %, respectively ($P < 0.05$, $n \geq 3$; Figure 4A, B). Confocal microscopy revealed a 39 % increase in $nNa_v1.5$ immunoreactivity towards the cell periphery defined by conA labelling, 8 days after RNAi treatment ($P < 0.05$, $n = 3$; Figure 4C).

In conclusion, the RNAi reduced *SCN1B* mRNA and β1 protein levels in MCF-7 cells, but increased $nNa_v1.5$ mRNA and protein levels.

3.3. Effects of β1 silencing on metastatic cell behaviours of MCF-7 cells

Adhesion—MCF-7 cells are significantly more adhesive to substrate than MDA-MB-231 cells (Palmer et al., 2008), consistent with the relatively higher level of *SCN1B* in the former (Figure 1) and the role of β1 as a CAM (Davis et al., 2004, Malhotra et al., 2000, Malhotra et al., 2002). Measurements of single-cell adhesion of *SCN1B* siRNA-treated MCF-7 cells revealed a significant reduction in adhesion of 25 % ($P < 0.05$; $n = 3$) and 35 % ($P < 0.001$; $n = 6$) after 5 and 8 days, respectively (Figure 5A). However, by 12 days post-transfection, when levels of *SCN1B* mRNA had returned to normal, the cells' adhesive capability had recovered such that there was no significant difference ($P = 0.13$; $n = 3$; Figure 5A), consistent with the interpretation that β1 normally functions as a CAM in these cells. Pre-treatment of cells for 48 h with TTX (10 μM, continued during the assay) increased the adhesion of control cells by 16 % ($P < 0.01$; $n = 4$; Figure 5B, bars 1 vs. 3). Similarly, TTX increased the adhesion of *SCN1B* siRNA-treated cells by 28 % ($P < 0.05$; $n = 4$; Figure 5B, bars 2 vs. 4). In conclusion, downregulation of β1 reduced adhesion of MCF-7 cells, and this effect was partially reversed by TTX.

Transwell migration—Eight days following transfection with siRNA targeting *SCN1B*, the number of migrating MCF-7 cells increased by 121 % ($P < 0.05$; $n = 8$; Figure 5C, bars 1 vs.

2), again suggesting that β1 normally functions as a CAM in these cells. Pre-treatment with TTX for 48 h (continued during the assay) reduced migration of siControl-treated cells by 27 % ($P < 0.05$; n = 8; Figure 5C, bars 1 vs. 3). Similarly, TTX also reduced migration of siRNA-treated cells by 43 % ($P < 0.05$; n = 8; Figure 5C, bars 2 vs. 4). Importantly, there was no difference in migration between TTX-pretreated siControl or siRNA-treated cells ($P > 0.05$, n = 8; Figure 5C, bars 3 vs. 4). TTX had no effect on *SCN1B* or *SCN4B* mRNA levels ($P = 0.85$ and $P = 0.70$, respectively; n = 3; Figure 5D), although *SCN2B* mRNA was reduced by 55 % ($P < 0.05$; n = 3; Figure 5D).

In conclusion, downregulation of β1 reduced adhesion but increased migration of MCF-7 cells. Both effects were sensitive to TTX, consistent with involvement of VGSC activity.

3.4 Effects of stably expressing β1 in MDA-MB-231 cells

β1 protein is detectable in MCF-7 cells, but not MDA-MB-231 cells (Figure 1). Further, MCF-7 cells exhibit enhanced adhesion and reduced migration compared to MDA-MB-231 cells, suggesting that β1 expression influences these properties (Figure 5). Thus, we next investigated whether overexpression of β1 in MDA-MB-231 cells might increase their adhesion and reduce cellular migration. eGFP-β1 was transfected into MDA-MB-231 cells and stable expression was monitored by epifluorescence (Figure 6A). For all experiments, the effects of β1 were compared with control cells expressing eGFP alone. Western blot analysis confirmed expression of eGFP protein (30 kDa) in the control cell line, and revealed the expected increase of 37 kDa in molecular weight of eGFP in cells expressing the β1-eGFP fusion protein (Figure 6B).

VGSC activity—Expression of β1 protein in MDA-MB-231 cells increased peak Na^+ current density by 34 %, from -34.5 ± 4.2 mV, to -46.4 ± 4.1 mV ($P < 0.05$; n = 20; Figure 7A, B, Table 2). In addition, β1 accelerated the kinetics of activation, reducing the time to reach peak current (T_p), from 0.73 ± 0.03 ms, to 0.65 ± 0.02 ms ($P < 0.05$; n = 20; Table 2). In contrast, the whole-cell capacitance, persistent current, voltage-dependence of activation and steady-state inactivation, time constants of inactivation, recovery from inactivation, and use-dependent rundown at 50 Hz were unchanged (Figure 7C-F, Table 2). In summary, β1 increased peak VGSC current density and reduced T_p, without affecting other Na+ current characteristics.

Morphology—The distribution of β1-eGFP fusion protein in transfected cells was detected throughout the cell body and processes, with high expression observed in perinuclear clusters (Figure 6A). β1-eGFP-transfected cells had significantly increased process length and this was observed in cells with both monopolar and biopolar morphologies ($P < 0.01$ for both; n = 40; Figure 8A). The thickness of processes on β1-eGFP-expressing monopolar cells was significantly reduced compared to cells expressing eGFP alone ($P < 0.01$; n = 40; Figure 8B). In contrast, the process thickness on bipolar cells was unchanged ($P = 0.46$; n = 40; Figure 8B). The cell body diameter of β1-eGFP-transfected cells was unchanged in both monopolar and bipolar cells compared to eGFP alone ($P = 0.26$ and 0.91, respectively; n = 40; Figure 8C). In conclusion, β1 overexpression appeared to increase process extension in MDA-MB-231 cells. While the mechanism of this effect is not clear for BCa cells, we have shown previously that β1-β1 cell adhesive interactions result in increased process length in neurons (Brackenbury et al., 2008a, Davis et al., 2004).

Adhesion—Cell-cell adhesion was measured using a cellular aggregation assay. β1-eGFP overexpression increased cell-cell adhesion of MDA-MB-231 cells compared to cells expressing eGFP alone following 30 min of shaking, and this effect persisted for 2 h ($P < 0.05$; n = 3; Figure 8D). This result is consistent with the proposed role for β1 in *trans*-homophilic cell adhesion, described previously (Malhotra et al., 2000).

Lateral motility and proliferation—The lateral motility of MDA-MB-231 cells was measured using a wound-heal assay. eGFP-β1 expression reduced the MI by 21 % from 0.68 ± 0.01 to 0.53 ± 0.01 compared to cells expressing eGFP alone ($P < 0.001$; $n > 320$; Figure 8E). In addition, the proliferation of cells expressing eGFP-β1 was reduced by 19 % compared to control ($P < 0.05$; $n = 3$; Figure 8F). These findings suggest that β1 expression may reduce wound closure by enhancing cell-cell or cell-matrix adhesion. However, the reduced proliferation of these cells may also have contributed to this effect.

4. Discussion

This study is the first investigation of the role of VGSC β1 subunits in BCa cells and provides new insights into the potential role of these multifunctional molecules in cancer metastasis. The main findings of this study are as follows: (i) Weakly metastatic MCF-7 cells expressed considerably higher levels of *SCN1B*, *SCN2B*, and *SCN4B* mRNAs than metastatic MDA-MB-231 cells. (ii) *SCN1B* was the most abundant VGSC β subunit mRNA expressed in both MCF-7 and MDA-MB-231 cell lines. (iii) β1 silencing experiments suggested that β1 normally increases adhesion and attenuates Transwell migration of MCF-7 cells. (iv) β1 silencing positively regulated $nNa_v1.5$ mRNA and plasma membrane protein levels in MCF-7 cells. (v) TTX partially reversed the effects of β1-silencing on adhesion and migration in MCF-7 cells, suggesting that VGSC expression and resulting changes in electrical activity may influence metastasis. A potential caveat to this interpretation is the observation that TTX reduced *SCN2B* mRNA expression. β2 has also been shown to play roles in cell adhesion *in vitro*, including attenuating neurite outgrowth and thus may also contribute to the observed changes in adhesion and migration. (vi) Overexpression of β1 in MDA-MB-231 cells increased Na^+ current density, cell process length, and cell-cell adhesion, and reduced cellular lateral motility and proliferation. Taken together, these results suggest that β1 expression enhances adhesiveness and attenuates migration of BCa cells. The cell adhesive effects of β1 overexpression in MDA-MD-231 cells were observed concomitantly with β1-mediated upregulation of Na^+ current density, suggesting that the cell adhesive effects of β1 may be independent of changes in excitability and supporting the notion that β1 may have autonomous functional roles independent of the ion-conducting pore (Brackenbury and Isom, 2008, Brackenbury et al., 2007). The regulation of $nNa_v1.5$ expression/activity by β1 silencing in MCF-7 cells further suggests that β1 may control VGSC-dependent electrical signal transduction in BCa.

4.1 Expression of β subunits in human BCa cell lines

We used RNAi to downregulate *SCN1B* in MCF-7 cells. The siRNAs reduced *SCN1B* mRNA by 75 % after 4 days, without affecting *SCN2B* or *SCN4B*. β1 protein levels were reduced to a lesser extent, by 40 % after 8 days. The reduced and delayed protein reduction could be due to incomplete downregulation of the target gene (Jackson et al., 2003). Although dynamics of α and β subunit mRNA/protein expression in cancer cells are not known, it is possible that large intracellular protein stores and/or slow turnover may also contribute to the difference in time course (Brackenbury et al., 2007, Li et al., 2004). Also, increasing evidence suggests that VGSC mRNA and protein levels do not correlate (Lopez-Santiago et al., 2006, Brackenbury and Djamgoz, 2006). Nonetheless, a small reduction in protein level can still result in significant functional changes. For example, 40-60 % silencing of $nNa_v1.5$ was enough to critically disrupt cancer cell migration (Brackenbury et al., 2007).

SCN4B mRNA was present in both MCF-7 and MDA-MB-231 cells in a longer and a shorter form. A similar situation has been found in a human prostate cancer cell line (LNCaP) (Diss et al., 2007). In addition, we found that *SCN3B* mRNA was not detectable in either MCF-7 or MDA-MB-231 cells. Given that the *SCN3B* gene contains two p53 response elements and may

be involved in p53-dependent apoptosis (Adachi et al., 2004), the absence of *SCN3B* in BCa cells may promote oncogenesis. This is an interesting possibility that would be worthy of further investigation.

4.2 Effect of VGSC activity on β subunit expression

TTX had no effect on *SCN1B* or *SCN4B* mRNA levels in MCF-7 cells. However, *SCN2B* mRNA expression was reduced by 55 %. Thus, β subunit expression appears dynamic and, in the case of *SCN2B*, may be controlled by α subunit activity. In agreement with this, electrical activity affects L1 CAM expression in mouse sensory neurons (Itoh et al., 1995). In addition, α subunit activity regulates *SCN9A* mRNA levels in metastatic PCa cells (Brackenbury and Djamgoz, 2006). Interestingly, VGSC α subunit mRNA levels are regulated by a cleavage product of β2 protein in neurons (Kim et al., 2007). Thus, VGSC α and β2 transcription and translation may be tightly and reciprocally regulated.

4.3 Regulation of metastatic cell behaviours by β1

Downregulation of β1 in MCF-7 cells reduced single-cell adhesion, while overexpression of β1 in MDA-MB-231 cells increased cell-cell adhesion and process length. These results are consistent with the hypothesis that β1 functions as a CAM in BCa cells. β1 participates in homophilic adhesion in vitro and in vivo, resulting in cellular aggregation, ankyrin recruitment, neurite outgrowth, fasciculation, and migration (Davis et al., 2004, Malhotra et al., 2002, Malhotra et al., 2000, Brackenbury et al., 2008a). In addition, given that β1 can interact with other CAMs, as well as the extracellular matrix protein tenascin-R (Malhotra et al., 2004, Kazarinova-Noyes et al., 2001, Xiao et al., 1999), it is likely that β1 could play a significant adhesive role in BCa. For example, contactin, known to interact with β1, is involved in invasion and metastasis of lung adenocarcinoma cells (McEwen et al., 2004, Brackenbury et al., 2008a, Su et al., 2006).

SCN1B siRNA increased the Transwell migration of MCF-7 cells. We propose that downregulation of β1 reduced the cells' adhesion, and in doing so, rendered them more capable of migration. Consistent with this result, overexpression of β1 in MDA-MB-231 cells reduced their lateral motility. As with the MCF-7 cells, β1 may reduce MDA-MB-231 motility via enhanced adhesion. However, β1 also reduced the proliferation of MDA-MB-231 cells, which could also contribute to the reduced MI. Thus, β1 may also regulate survival and/or proliferation of MDA-MB-231 cells by as yet, unidentified mechanism(s).

Interestingly, TTX partially reversed the effects of *SCN1B* silencing on the adhesion and migration of MCF-7 cells. Thus, the reduction in adhesion, and increase in migration in the absence of β1 is, at least in part, dependent on α subunit activity. TTX has been shown to inhibit a variety of behaviours associated with the metastatic cascade (reviewed in Brackenbury et al., 2008b). It is possible that metastatic cell behaviours dependent on α subunit activity may also require concomitant downregulation of β1.

4.4. Regulation of nNa_v1.5 functional expression by β1

Overexpression of β1 in MDA-MB-231 cells increased Na^+ current density and reduced T_p. The effects of β1 on Na_v1.5, the predominant α subunit expressed in MDA-MB-231 cells (Fraser et al., 2005), appear to be controversial, and dependent on the cell type studied. Consistent with the present findings, some studies report that β1 increases Na_v1.5 current density without affecting gating (Nuss et al., 1995, Qu et al., 1995). However, other reports suggest that β1 does not affect Na_v1.5 function (Makita et al., 1994, Yang et al., 1993), or shifts voltage-dependence of steady-state inactivation (An et al., 1998, Malhotra et al., 2001), or affects recovery from inactivation (Fahmi et al., 2001). In contrast to these previous studies, Na_v1.5 is primarily expressed in MDA-MB-231 cells as the D1:S3 nNa_v1.5 splice variant

(Brackenbury et al., 2007, Fraser et al., 2005). Given that $nNa_v1.5$ exhibits subtly different gating and kinetics compared to the 'adult' splice variant (Onkal et al., 2008), it is possible that β1 may modulate $nNa_v1.5$ in a different manner.

Downregulation of β1 in MCF-7 cells resulted in upregulation of $nNa_v1.5$ mRNA and protein. *Scn1b* null mice have increased *Scn5a* mRNA and $Na_v1.5$ protein in cardiomyocytes (Lopez-Santiago et al., 2007). Therefore, β1 may be a novel regulator of *Scn5a*/$Na_v1.5$ expression in multiple tissues. Emerging evidence suggests that β subunits may function as transcription factors. For example, β subunits can be cleaved by secretases, yielding functional intracellular domains (ICDs) (Wong et al., 2005, Kim et al., 2005). In the case of β2, the ICD increases *Scn1a* mRNA and $Na_v1.1$ protein levels (Kim et al., 2007). The β1-ICD may normally participate in repression of *SCN5A* transcription, such that the *SCN1B* null mutation results in *SCN5A* overexpression. In an alternative scenario, β1 in MCF-7 cells may serve to negatively regulate $nNa_v1.5$ expression indirectly, via adhesion. Downregulation of β1 would reduce the cells' adhesion, in turn enhancing metastatic behaviours including migration, concomitant with $nNa_v1.5$ upregulation. $nNa_v1.5$ is primarily responsible for the VGSC-dependent enhancement of invasive behaviour in metastatic MDA-MB-231 cells (Brackenbury et al., 2007). The mechanism(s) underlying α subunit upregulation in metastatic cancer cells is not understood, although serum and growth factors are important (Pan and Djamgoz, 2008, Onganer and Djamgoz, 2007, Ding et al., 2008, Ding and Djamgoz, 2004, Brackenbury and Djamgoz, 2007). Given that β1 increased Na^+ current density in MDA-MB-231 cells, but reduced lateral motility, this would suggest that the steady-state contribution of basal α subunit activity to enhancing motility in MDA-MB-231 cells is maximal. However, it is not yet clear whether $nNa_v1.5$ expression is required for the acquisition of metastatic capability, or whether it is upregulated once the BCa cells have become highly metastatic.

4.5 Concluding remarks

This work further supports the proposed role of VGSCs in the cancer process and may have important clinical implications. Loss of β1 expression in line with acquisition of metastatic capability may provide a novel prognostic marker for BCa progression (Brackenbury and Isom, 2008). Furthermore, β1 may provide a target for gene therapy, whereby its overexpression could enhance adhesion, resulting in reduction of metastatic cell behaviour in BCa.

Acknowledgements

Financial support was from a Pro Cancer Research Fund (PCRF) Amber Fellowship to A-MC, a University of Michigan Center for Organogenesis Non-Traditional Postdoctoral Fellowship to WJB, and NIH R01MH059980 grant to LLI. Further support was provided by the Leventis Foundation (A-MC). We would like to thank Dr James Diss for advice on real-time PCR experiments, Dongmin Shao, Rustem Onkal and Jeffrey Little for technical assistance, and Dr Kenji Okuse for commenting on the manuscript.

References

Adachi K, Toyota M, Sasaki Y, Yamashita T, Ishida S, Ohe-Toyota M, Maruyama R, Hinoda Y, Saito T, Imai K, Kudo R, Tokino T. Identification of SCN3B as a novel p53-inducible proapoptotic gene. Oncogene 2004;23:7791–7798. [PubMed: 15334053]

Allen DH, Lepple-Wienhues A, Cahalan MD. Ion channel phenotype of melanoma cell lines. J Membr Biol 1997;155:27–34. [PubMed: 9002422]

An RH, Wang XL, Kerem B, Benhorin J, Medina A, Goldmit M, Kass RS. Novel LQT-3 mutation affects Na^+ channel activity through interactions between alpha-and beta1-subunits. Circ Res 1998;83:141–146. [PubMed: 9686753]

Armstrong CM, Bezanilla F. Inactivation of the sodium channel. II. Gating current experiments. J Gen Physiol 1977;70:567–590. [PubMed: 591912]

Bennett ES, Smith BA, Harper JM. Voltage-gated Na^+ channels confer invasive properties on human prostate cancer cells. Pflugers Arch 2004;447:908–914. [PubMed: 14677067]

Brackenbury WJ, Chioni AM, Diss JK, Djamgoz MB. The neonatal splice variant of Nav1.5 potentiates in vitro metastatic behaviour of MDA-MB-231 human breast cancer cells. Breast Cancer Res Treat 2007;101:149–160. [PubMed: 16838113]

Brackenbury WJ, Davis TH, Chen C, Slat EA, Detrow MJ, Dickendesher TL, Ranscht B, Isom LL. Voltage-gated Na^+ channel β1 subunit-mediated neurite outgrowth requires fyn kinase and contributes to central nervous system development in vivo. J Neurosci 2008a;28:3246–3256. [PubMed: 18354028]

Brackenbury WJ, Djamgoz MB. Activity-dependent regulation of voltage-gated Na^+ channel expression in Mat-LyLu rat prostate cancer cell line. J Physiol 2006;573(Pt 2):343–356. [PubMed: 16543264]

Brackenbury WJ, Djamgoz MB. Nerve growth factor enhances voltage-gated Na^+ channel activity and transwell migration in Mat-LyLu rat prostate cancer cell line. J Cell Physiol 2007;210:602–608. [PubMed: 17149708]

Brackenbury WJ, Djamgoz MB, Isom LL. An emerging role for voltage-gated Na^+ channels in cellular migration: Regulation of central nervous system development and potentiation of invasive cancers. The Neuroscientist. 2008b10.1177/1073858408320293

Brackenbury WJ, Isom LL. Voltage-gated Na^+ channels: potential for beta subunits as therapeutic targets. Expert Opin Ther Targets 2008;12:1191–1203. [PubMed: 18694383]

Catterall WA. Cellular and molecular biology of voltage-gated sodium channels. Physiol Rev 1992;72:S15–48. [PubMed: 1332090]

Catterall WA. From ionic currents to molecular mechanisms: the structure and function of voltage-gated sodium channels. Neuron 2000;26:13–25. [PubMed: 10798388]

Chioni AM, Fraser SP, Pani F, Foran P, Wilkin GP, Diss JK, Djamgoz MB. A novel polyclonal antibody specific for the $Na_V1.5$ voltage-gated Na^+ channel 'neonatal' splice form. J Neurosci Methods 2005;147:88–98. [PubMed: 16111763]

Davis TH, Chen C, Isom LL. Sodium channel β1 subunits promote neurite outgrowth in cerebellar granule neurons. J Biol Chem 2004;279:51424–51432. [PubMed: 15452131]

Diaz D, Delgadillo D, Hernandez-Gallegoz E, Ramirez-Dominguez M, Hinojosa L, Ortiz C, Berumen J, Camacho J, Gomora J. Functional expression of voltage-gated sodium channels in primary cultures of human cervical cancer. J Cell Physiol 2007;210:469–478. [PubMed: 17051596]

Ding Y, Brackenbury WJ, Onganer PU, Montano X, Porter LM, Bates LF, Djamgoz MB. Epidermal growth factor upregulates motility of Mat-LyLu rat prostate cancer cells partially via voltage-gated Na^+ channel activity. J Cell Physiol 2008;215:77–81. [PubMed: 17960590]

Ding Y, Djamgoz MB. Serum concentration modifies amplitude and kinetics of voltage-gated Na^+ current in the Mat-LyLu cell line of rat prostate cancer. Int J Biochem Cell Biol 2004;36:1249–1260. [PubMed: 15109569]

Diss JK, Archer SN, Hirano J, Fraser SP, Djamgoz MB. Expression profiles of voltage-gated Na^+ channel alpha-subunit genes in rat and human prostate cancer cell lines. Prostate 2001;48:165–178. [PubMed: 11494332]

Diss JK, Fraser SP, Walker MM, Patel A, Latchman DS, Djamgoz MB. beta-Subunits of voltage-gated sodium channels in human prostate cancer: quantitative in vitro and in vivo analyses of mRNA expression. Prostate Cancer Prostatic Dis. 200710.1038/sj.pcan.4501012

Diss JK, Stewart D, Pani F, Foster CS, Walker MM, Patel A, Djamgoz MB. A potential novel marker for human prostate cancer: voltage-gated sodium channel expression in vivo. Prostate Cancer Prostatic Dis 2005;8:266–273. [PubMed: 16088330]

Djamgoz MBA, Mycielska M, Madeja Z, Fraser SP, Korohoda W. Directional movement of rat prostate cancer cells in direct-current electric field: involvement of voltage gated Na^+ channel activity. J Cell Sci 2001;114:2697–2705. [PubMed: 11683396]

Fahmi AI, Patel M, Stevens EB, Fowden AL, John JE 3rd, Lee K, Pinnock R, Morgan K, Jackson AP, Vandenberg JI. The sodium channel beta-subunit SCN3b modulates the kinetics of SCN5a and is expressed heterogeneously in sheep heart. J Physiol 2001;537:693–700. [PubMed: 11744748]

Fein AJ, Wright MA, Slat EA, Ribera AB, Isom LL. *scn1bb*, a zebrafish ortholog of *SCN1B* expressed in excitable and non-excitable cells, affects motor neuron axon morphology and touch sensitivity. J Neurosci. 2008In press

Fraser SP, Ding Y, Liu A, Foster CS, Djamgoz MB. Tetrodotoxin suppresses morphological enhancement of the metastatic MAT-LyLu rat prostate cancer cell line. Cell Tissue Res 1999;295:505–512. [PubMed: 10022970]

Fraser SP, Diss JK, Chioni AM, Mycielska M, Pan H, Yamaci RF, Pani F, Siwy Z, Krasowska M, Grzywna Z, Brackenbury WJ, Theodorou D, Koyuturk M, Kaya H, Battaloglu E, Tamburo De Bella M, Slade MJ, Tolhurst R, Palmieri C, Jiang J, Latchman DS, Coombes RC, Djamgoz MB. Voltage-gated sodium channel expression and potentiation of human breast cancer metastasis. Clin Cancer Res 2005;11:5381–5389. [PubMed: 16061851]

Fraser SP, Diss JK, Lloyd LJ, Pani F, Chioni AM, George AJ, Djamgoz MB. T-lymphocyte invasiveness: control by voltage-gated Na^+ channel activity. FEBS Lett 2004;569:191–194. [PubMed: 15225632]

Fraser SP, Salvador V, Manning EA, Mizal J, Altun S, Raza M, Berridge RJ, Djamgoz MB. Contribution of functional voltage-gated Na^+ channel expression to cell behaviors involved in the metastatic cascade in rat prostate cancer: I. lateral motility. J Cell Physiol 2003;195:479–487. [PubMed: 12704658]

Fulgenzi G, Graciotti L, Faronato M, Soldovieri MV, Miceli F, Amoroso S, Annunziato L, Procopio A, Taglialatela M. Human neoplastic mesothelial cells express voltage-gated sodium channels involved in cell motility. Int J Biochem Cell Biol 2006;38:1146–1159. [PubMed: 16458569]

Grimes JA, Fraser SP, Stephens GJ, Downing JE, Laniado ME, Foster CS, Abel PD, Djamgoz MB. Differential expression of voltage-activated Na^+ currents in two prostatic tumour cell lines: contribution to invasiveness in vitro. FEBS Lett 1995;369:290–294. [PubMed: 7649275]

Isom LL. Sodium channel β subunits: anything but auxiliary. The Neuroscientist 2001;7:42–54. [PubMed: 11486343]

Isom LL, De Jongh KS, Catterall WA. Auxiliary subunits of voltage-gated ion channels. Neuron 1994;12:1183–1194. [PubMed: 7516685]

Isom LL, De Jongh KS, Patton DE, Reber BF, Offord J, Charbonneau H, Walsh K, Goldin AL, Catterall WA. Primary structure and functional expression of the beta 1 subunit of the rat brain sodium channel. Science 1992;256:839–842. [PubMed: 1375395]

Isom LL, Ragsdale DS, De Jongh KS, Westenbroek RE, Reber BF, Scheuer T, Catterall WA. Structure and function of the beta 2 subunit of brain sodium channels, a transmembrane glycoprotein with a CAM motif. Cell 1995;83:433–442. [PubMed: 8521473]

Itoh K, Stevens B, Schachner M, Fields RD. Regulated expression of the neural cell adhesion molecule L1 by specific patterns of neural impulses. Science 1995;270:1369–1372. [PubMed: 7481827]

Jackson AL, Bartz SR, Schelter J, Kobayashi SV, Burchard J, Mao M, Li B, Cavet G, Linsley PS. Expression profiling reveals off-target gene regulation by RNAi. Nat Biotechnol 2003;21:635–637. [PubMed: 12754523]

Kazarinova-Noyes K, Malhotra JD, McEwen DP, Mattei LN, Berglund EO, Ranscht B, Levinson SR, Schachner M, Shrager P, Isom LL, Xiao Z-C. Contactin associates with Na^+ channels and increases their functional expression. J Neurosci 2001;21:7517–7525. [PubMed: 11567041]

Kim DY, Carey BW, Wang H, Ingano LA, Binshtok AM, Wertz MH, Pettingell WH, He P, Lee VM, Woolf CJ, Kovacs DM. BACE1 regulates voltage-gated sodium channels and neuronal activity. Nat Cell Biol 2007;9:755–764. [PubMed: 17576410]

Kim DY, Mackenzie Ingano LA, Carey BW, Pettingell WP, Kovacs DM. Presenilin/gamma -secretase-mediated cleavage of the voltage-gated sodium channel beta 2 subunit regulates cell adhesion and migration. J Biol Chem 2005;280:23251–23261. [PubMed: 15833746]

Laniado ME, Lalani EN, Fraser SP, Grimes JA, Bhangal G, Djamgoz MB, Abel PD. Expression and functional analysis of voltage-activated Na^+ channels in human prostate cancer cell lines and their contribution to invasion in vitro. Am J Pathol 1997;150:1213–1221. [PubMed: 9094978]

Li T, Chang CY, Jin DY, Lin PJ, Khvorova A, Stafford DW. Identification of the gene for vitamin K epoxide reductase. Nature 2004;427:541–544. [PubMed: 14765195]

Livak KJ, Schmittgen TD. Analysis of relative gene expression data using real-time quantitative PCR and the 2^{-ddCt} method. Methods 2001;25:402–408. [PubMed: 11846609]

Lopez-Santiago LF, Meadows LS, Ernst SJ, Chen C, Malhotra JD, McEwen DP, Speelman A, Noebels JL, Maier SK, Lopatin AN, Isom LL. Sodium channel Scn1b null mice exhibit prolonged QT and RR intervals. J Mol Cell Cardiol 2007;43:636–647. [PubMed: 17884088]

Lopez-Santiago LF, Pertin M, Morisod X, Chen C, Hong S, Wiley J, Decosterd I, Isom LL. Sodium channel beta2 subunits regulate tetrodotoxin-sensitive sodium channels in small dorsal root ganglion neurons and modulate the response to pain. J Neurosci 2006;26:7984–7994. [PubMed: 16870743]

Makita N, Bennett PB Jr, George AL Jr. Voltage-gated Na+ channel beta 1 subunit mRNA expressed in adult human skeletal muscle, heart, and brain is encoded by a single gene. J Biol Chem 1994;269:7571–7578. [PubMed: 8125980]

Malhotra J, Chen C, Rivolta I, Abriel H, Malhotra R, Mattei LN, Brosius FC, Kass RS, Isom LL. Characterization of sodium channel alpha-and beta-subunits in rat and mouse cardiac myocytes. Circulation 2001;103:1303–1310. [PubMed: 11238277]

Malhotra JD, Kazen-Gillespie K, Hortsch M, Isom LL. Sodium channel β subunits mediate homophilic cell adhesion and recruit ankyrin to points of cell-cell contact. J Biol Chem 2000;275:11383–11388. [PubMed: 10753953]

Malhotra JD, Koopmann MC, Kazen-Gillespie KA, Fettman N, Hortsch M, Isom LL. Structural requirements for interaction of sodium channel β1 subunits with ankyrin. J Biol Chem 2002;277:26681–26688. [PubMed: 11997395]

Malhotra JD, Thyagarajan V, Chen C, Isom LL. Tyrosine-phosphorylated and nonphosphorylated sodium channel beta1 subunits are differentially localized in cardiac myocytes. J Biol Chem 2004;279:40748–40754. [PubMed: 15272007]

McEwen DP, Meadows LS, Chen C, Thyagarajan V, Isom LL. Sodium channel β1 subunit-mediated modulation of Nav1.2 currents and cell surface density is dependent on interactions with contactin and ankyrin. J Biol Chem 2004;279:16044–16049. [PubMed: 14761957]

Morgan K, Stevens EB, Shah B, Cox PJ, Dixon AK, Lee K, Pinnock RD, Hughes J, Richardson PJ, Mizuguchi K, Jackson AP. beta 3: an additional auxiliary subunit of the voltage-sensitive sodium channel that modulates channel gating with distinct kinetics. Proc Natl Acad Sci U S A 2000;97:2308–2313. [PubMed: 10688874]

Nuss HB, Chiamvimonvat N, Perez-Garcia MT, Tomaselli GF, Marban E. Functional association of the beta 1 subunit with human cardiac (hH1) and rat skeletal muscle (mu 1) sodium channel alpha subunits expressed in Xenopus oocytes. J Gen Physiol 1995;106:1171–1191. [PubMed: 8786355]

Onganer PU, Djamgoz MB. Small-cell lung cancer (human): potentiation of endocytic membrane activity by voltage-gated Na^+ channel expression in vitro. J Membr Biol 2005;204:67–75. [PubMed: 16151702]

Onganer PU, Djamgoz MB. Epidermal growth factor potentiates in vitro metastatic behaviour of human prostate cancer PC-3M cells: Involvement of voltage-gated sodium channel. Mol Cancer 2007;6:76. [PubMed: 18036246]

Onganer PU, Seckl MJ, Djamgoz MB. Neuronal characteristics of small-cell lung cancer. Br J Cancer 2005;93:1197–1201. [PubMed: 16265346]

Onkal R, Mattis JH, Fraser SP, Diss JK, Shao D, Okuse K, Djamgoz MB. Alternative splicing of Nav1.5: An electrophysiological comparison of ‘neonatal’ and ‘adult’ isoforms and critical involvement of a lysine residue. J Cell Physiol 2008;216:716–726. [PubMed: 18393272]

Ou SW, Kameyama A, Hao LY, Horiuchi M, Minobe E, Wang WY, Makita N, Kameyama M. Tetrodotoxin-resistant Na^+ channels in human neuroblastoma cells are encoded by new variants of Nav1.5/SCN5A. Eur J Neurosci 2005;22:793–801. [PubMed: 16115203]

Palmer CP, Mycielska ME, Burcu H, Osman K, Collins T, Beckerman R, Perrett R, Johnson H, Aydar E, Djamgoz MB. Single cell adhesion measuring apparatus (SCAMA): application to cancer cell lines of different metastatic potential and voltage-gated Na^+ channel expression. Eur Biophys J 2008;37:359–368. [PubMed: 17879092]

Pan H, Djamgoz MB. Biochemical constitution of extracellular medium is critical for control of human breast cancer MDA-MB-231 cell motility. J Membr Biol 2008;223:27–36. [PubMed: 18575796]

Qu Y, Isom LL, Westenbroek RE, Rogers JC, Tanada TN, McCormick KA, Scheuer T, Catterall WA. Modulation of cardiac Na^+ channel expression in Xenopus oocytes by beta 1 subunits. J Biol Chem 1995;270:25696–25701. [PubMed: 7592748]

Ratcliffe CF, Qu Y, McCormick KA, Tibbs VC, Dixon JE, Scheuer T, Catterall WA. A sodium channel signaling complex: modulation by associated receptor protein tyrosine phosphatase beta. Nat Neurosci 2000;3:437–444. [PubMed: 10769382]

Roger S, Besson P, Le Guennec JY. Involvement of a novel fast inward sodium current in the invasion capacity of a breast cancer cell line. Biochim Biophys Acta 2003;1616:107–111. [PubMed: 14561467]

Roger S, Rollin J, Barascu A, Besson P, Raynal PI, Iochmann S, Lei M, Bougnoux P, Gruel Y, Le Guennec JY. Voltage-gated sodium channels potentiate the invasive capacities of human non-small-cell lung cancer cell lines. Int J Biochem Cell Biol 2007;39:774–786. [PubMed: 17307016]

Srinivasan J, Schachner M, Catterall WA. Interaction of voltage-gated sodium channels with the extracellular matrix molecules tenascin-C and tenascin-R. Proc Natl Acad Sci U S A 1998;95:15753–15757. [PubMed: 9861042]

Su JL, Yang CY, Shih JY, Wei LH, Hsieh CY, Jeng YM, Wang MY, Yang PC, Kuo ML. Knockdown of contactin-1 expression suppresses invasion and metastasis of lung adenocarcinoma. Cancer Res 2006;66:2553–2561. [PubMed: 16510572]

Wong HK, Sakurai T, Oyama F, Kaneko K, Wada K, Miyazaki H, Kurosawa M, De Strooper B, Saftig P, Nukina N. beta subunits of voltage-gated sodium channels are novel substrates of BACE1 and gamma - secretase. J Biol Chem 2005;280:23009–23017. [PubMed: 15824102]

Wong MH, Filbin MT. Dominant-negative effect on adhesion by myelin Po protein truncated in its cytoplasmic domain. J Cell Biol 1996;134:1531–1541. [PubMed: 8830780]

Xiao ZC, Ragsdale DS, Malhotra JD, Mattei LN, Braun PE, Schachner M, Isom LL. Tenascin-R is a functional modulator of sodium channel beta subunits. J Biol Chem 1999;274:26511–26517. [PubMed: 10473612]

Yang JS, Bennett PB, Makita N, George AL, Barchi RL. Expression of the sodium channel beta 1 subunit in rat skeletal muscle is selectively associated with the tetrodotoxin-sensitive alpha subunit isoform. Neuron 1993;11:915–922. [PubMed: 8240813]

Yu FH, Westenbroek RE, Silos-Santiago I, McCormick KA, Lawson D, Ge P, Ferriera H, Lilly J, DiStefano PS, Catterall WA, Scheuer T, Curtis R. Sodium channel beta4, a new disulfide-linked auxiliary subunit with similarity to beta2. J Neurosci 2003;23:7577–7585. [PubMed: 12930796]

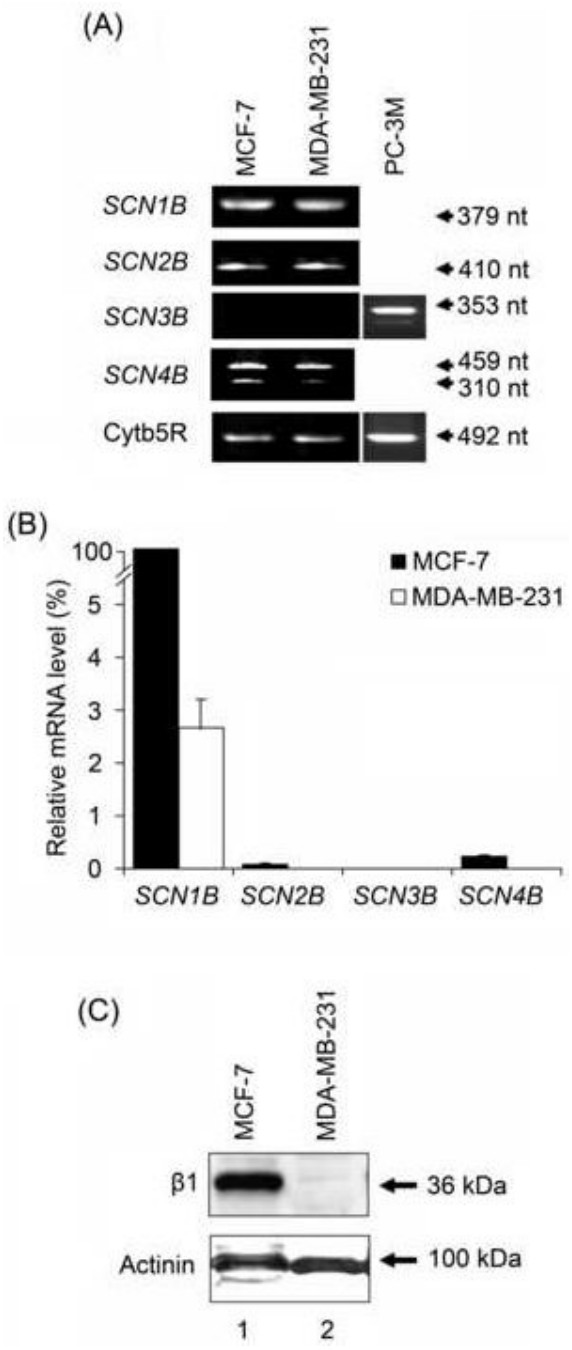

Figure 1. β subunit expression in MCF-7 and MDA-MB-231 cells

(A) Typical gel images of PCR products, taken at the end of the PCR, for *SCN1B*, *SCN2B*, *SCN3B*, *SCN4B* and cytochrome b5-reductase (Cytb5R) from MCF-7, MDA-MB-231 and PC-3M cells. The PC-3M cell line was used as a positive control for *SCN3B* expression (Diss et al., 2007). (B) Relative mRNA levels of *SCN1B*, *SCN2B*, *SCN3B* and *SCN4B*, normalised to Cytb5R by the $2^{-\Delta\Delta Ct}$ method, and expressed as a percentage of the *SCN1B* mRNA level in MCF-7 cells (fixed as 100 %). Each histobar indicates mean + error propagated through the $2^{-\Delta\Delta Ct}$ analysis (n = 3). Significance is shown in Table 1. (C) Western blot with 70 μg of total protein per lane from MCF-7 and MDA-MB-231 cells, using $\beta 1_{ex}$ and an actinin antibody as a control for loading. The same membrane was stripped and re-blotted.

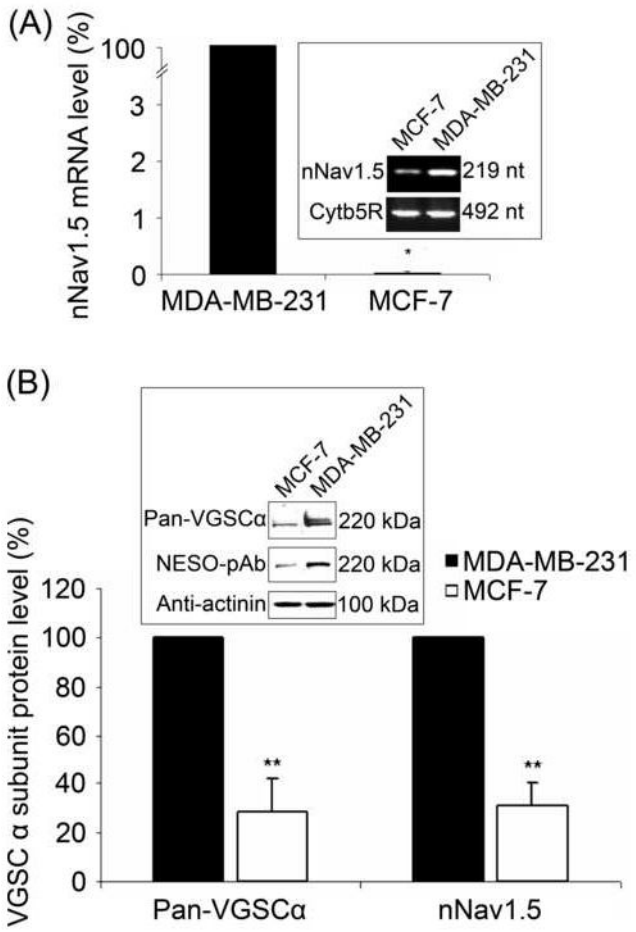

Figure 2. Expression of $nNa_v1.5$ mRNA and protein in MCF-7 and MDA-MB-231 cells

(A) Relative mRNA levels of $nNa_v1.5$, normalised to cytochrome b5-reductase (Cytb5R) by the $2^{-\Delta\Delta Ct}$ method, and expressed as a percentage of the level in MDA-MB-231 cells (fixed as 100 %). Errors are propagated through the $2^{-\Delta\Delta Ct}$ analysis (n = 4). Inset, typical gel images of $nNa_v1.5$ and Cytb5R real-time PCR products, taken at the end of the PCR. (B) Relative $nNa_v1.5$ and total VGSC α subunit protein levels in MDA-MB-231 and MCF-7 cells. For each antigen, the expression level in MDA-MB-231 cells was fixed as 100 %. The signal from NESO-pAb or pan-α subunit antibodies was normalised to the actinin control. Inset, Western blot with 60 μg of total protein per lane from MCF-7 and MDA-MB-231 cells, using NESO-pAb, pan-VGSC α subunit antibody, and actinin antibody as a control for loading. The same membrane was stripped and re-blotted. Each histobar indicates mean + SEM (n = 6). Significance: (*) $P < 0.05$, (**) $P < 0.01$; Mann-Whitney Rank Sum test.

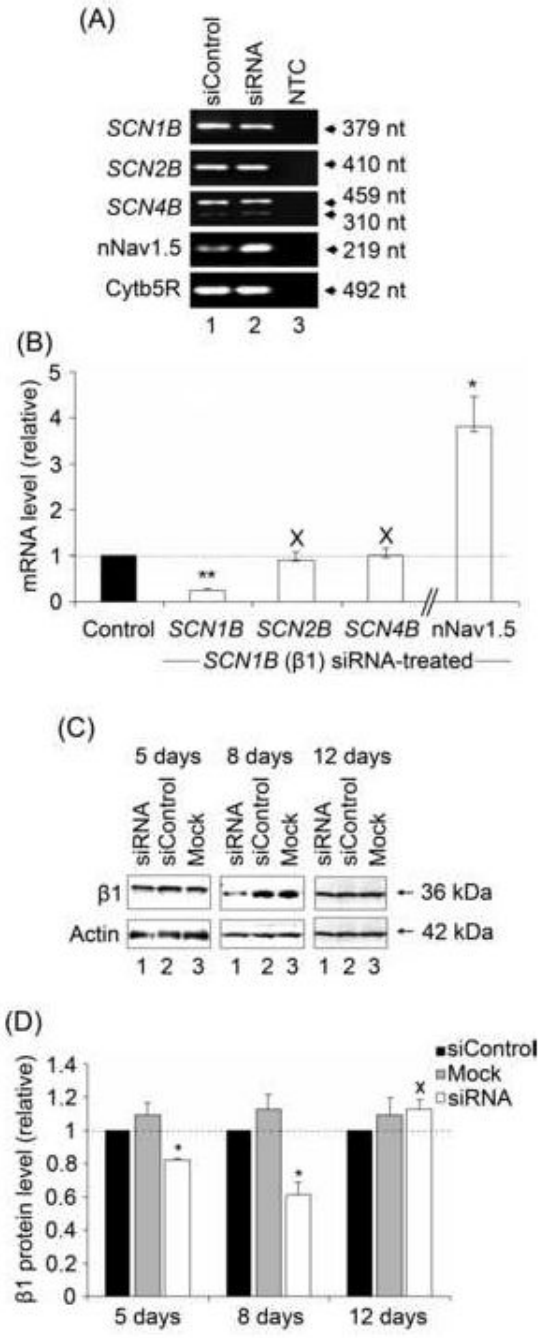

Figure 3. Effects of silencing *SCN1B* on VGSC expression in MCF-7 cells

(A) Typical gel images of PCR products, taken at the end of the PCR, for *SCN1B*, *SCN2B*, *SCN4B*, $nNa_v1.5$ and cytochrome-b5 reductase (Cytb5R) from MCF-7 cells 4 days after transfection with siControl (lane 1), or siRNA targeting *SCN1B* (lane 2). NTC (lane 3), no-template controls for PCR amplification. (B) Relative (%) mRNA levels of *SCN1B*, *SCN2B*, *SCN4B* and $nNa_v1.5$. Control (black bar – 100 %): MCF-7 cells treated with siControl non-targeting RNAi; white bars: MCF-7 cells treated with siRNA targeting *SCN1B*. β subunit and $nNa_v1.5$ mRNA levels were normalised to Cytb5R by the $2^{-\Delta\Delta Ct}$ method. Errors are propagated through the $2^{-\Delta\Delta Ct}$ analysis (n = 3). (C) Western blots with 70 μg of total protein per lane from cells 5, 8 and 12 days after treatment. For each case, lane 1, treatment with 'mock' control (no

siRNA); lane 2, treatment with non-targeting siControl siRNA; and lane 3, treatment with siRNA targeting *SCN1B*. The $\beta 1_{ex}$ antibody and an anti-actin antibody were used for β1 and for loading control, respectively (the same membrane was stripped and re-blotted). (D) Quantification of the data shown in (C). Relative total β1 protein levels were normalised to the actin control. Data are presented as mean and SEM ($n \geq 4$). Significance: (X) $P > 0.05$; (*) $P < 0.05$; (**) $P < 0.01$; ANOVA with Newman-Keuls (B), Student's paired t-test (D).

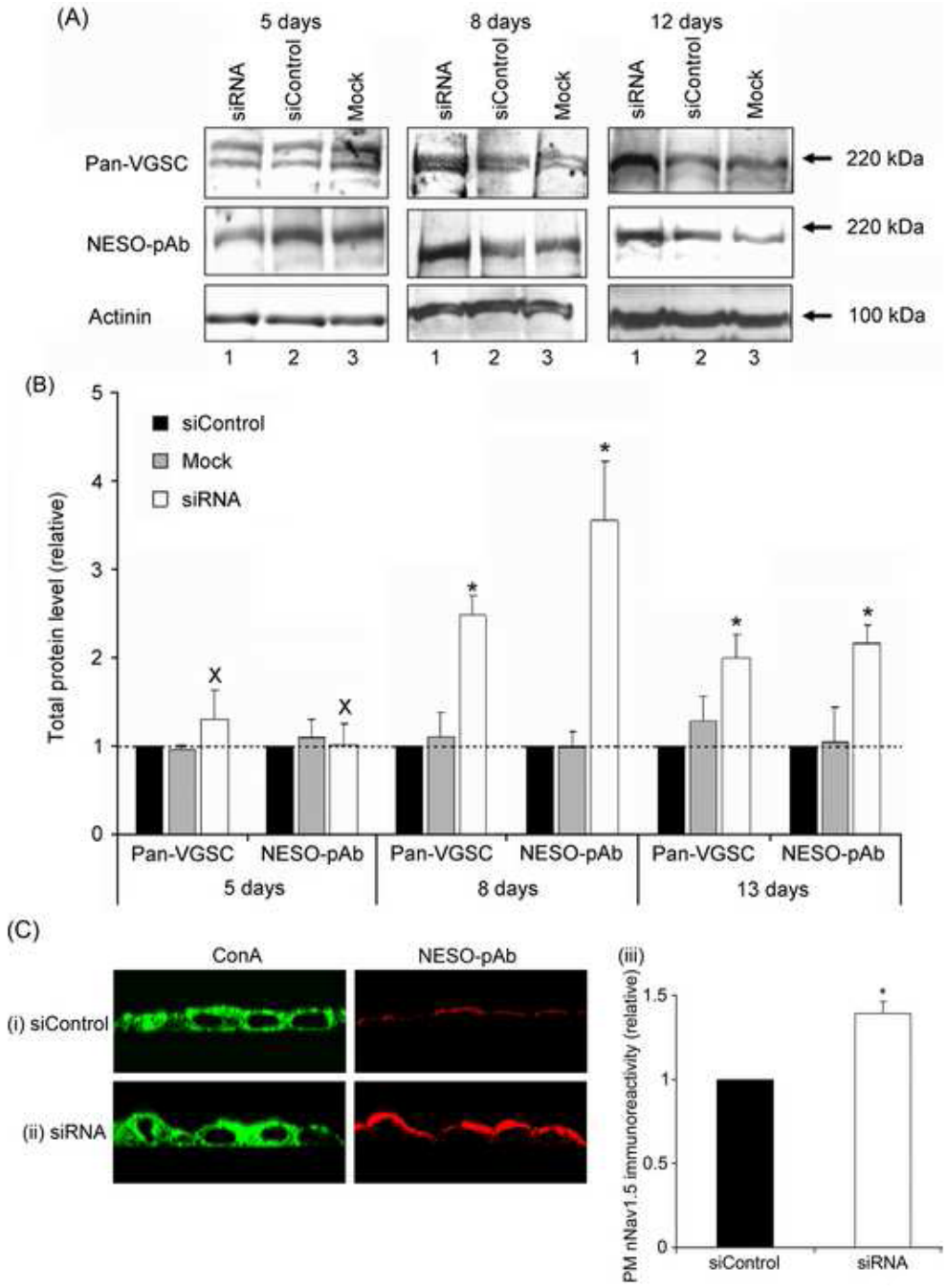

Figure 4. Effect of RNAi targeting *SCN1B* on the nNa$_v$1.5 protein level in MCF-7 cells

(A) Western blots with 80 μg of total protein per lane from cells 5, 8 and 12 days after treatment. For each case, lane 1, treatment with 'mock' control (no siRNA); lane 2, treatment with non-targeting siControl siRNA; and lane 3, treatment with siRNA targeting *SCN1B*. Antibodies used were pan-VGSC (for total VGSC), NESO-pAb for nNa$_v$1.5 and an actinin antibody for loading control. The same membrane was stripped and re-blotted. (B) Quantification of the data shown in (A). Relative total VGSC α subunit and nNa$_v$1.5 protein levels normalised to the actinin control. (C) Typical confocal XZY images of non-permeablised MCF-7 cells 8 days after transfection with (i) non-targeting siControl siRNA or (ii) siRNA targeting *SCN1B* double-immunolabelled with conA plasma membrane marker (left) and NESO-pAb (right);

(iii), Relative peripheral n$Na_V1.5$ level, measured from the confocal XZY images. Data are presented as mean and SEM [(B), n = 4; (C), n = 3]. Significance: (*) $P < 0.05$; (B), ANOVA with Newman-Keuls; (C) Student's paired t-test.

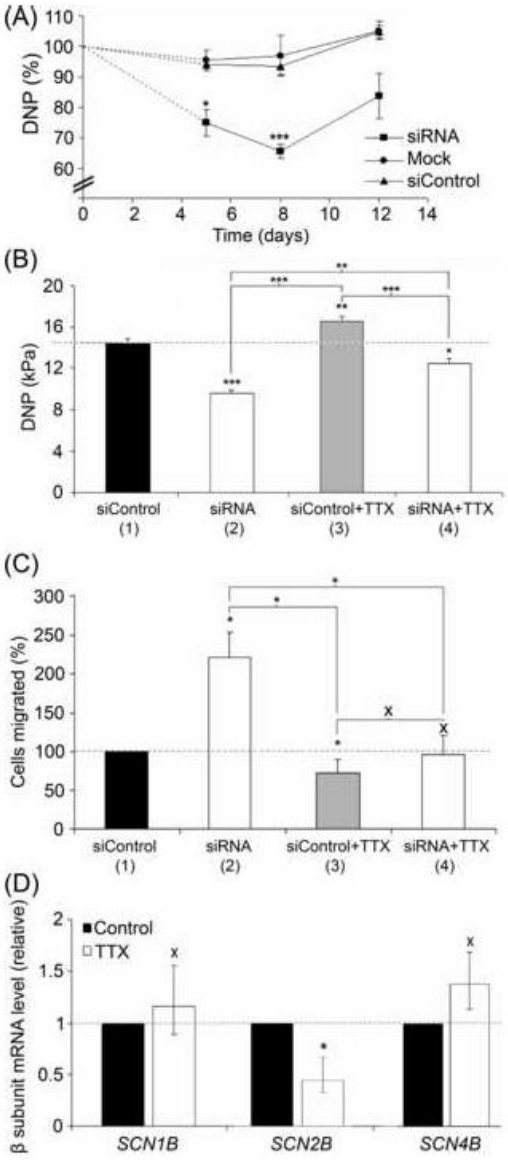

Figure 5. Effects of β1 downregulation on adhesion and migration of MCF-7 cells

(A) Time-course of reduction in relative detachment negative pressure (DNP) of MCF-7 cells following transfection with siRNA targeting *SCN1B*. Circles, 'mock' control (without siRNA); triangles, siControl non-targeting siRNA; squares, siRNA targeting *SCN1B*. (B) Absolute DNP values (in kPa) of MCF-7 cells 8 days after transfection with siControl non-targeting siRNA (bar 1) or siRNA targeting *SCN1B* (bar 2). In a separate experiment, cells were pre-treated with TTX (10 μM for 48 h), continued during the assay for cells transfected with siControl non-targeting siRNA (bar 3) or siRNA targeting β1(bar 4). (C) Relative number of cells migrating through a Transwell chamber over 12 h, 8 days after transfection with siControl non-targeting siRNA (bar 1) or siRNA targeting *SCN1B* (bar 2). In a separate experiment, cells were pre-treated with TTX (10 μM for 48 h), continued during the assay for cells transfected with siControl non-targeting siRNA (bar 3) or siRNA targeting *SCN1B* (bar 4). (D) Relative mRNA levels of *SCN1B*, *SCN2B* AND *SCN4B* in MCF-7 cells after 48 hours treatment with/without TTX (10 μM), normalised to cytochrome b5-reductase (Cytb5R) by the $2^{-\Delta\Delta Ct}$ method. Errors are propagated through the $2^{-\Delta\Delta Ct}$ analysis (n = 3). Data in (A), (B) and (C) are presented as

mean ± SEM ($n \geq 3$). Significance: (X) $P > 0.05$; (*) $P < 0.05$, (**) $P < 0.01$, (***) $P < 0.001$; (A), (B), (C) ANOVA with Newman-Keuls; (D) Student's paired t-test.

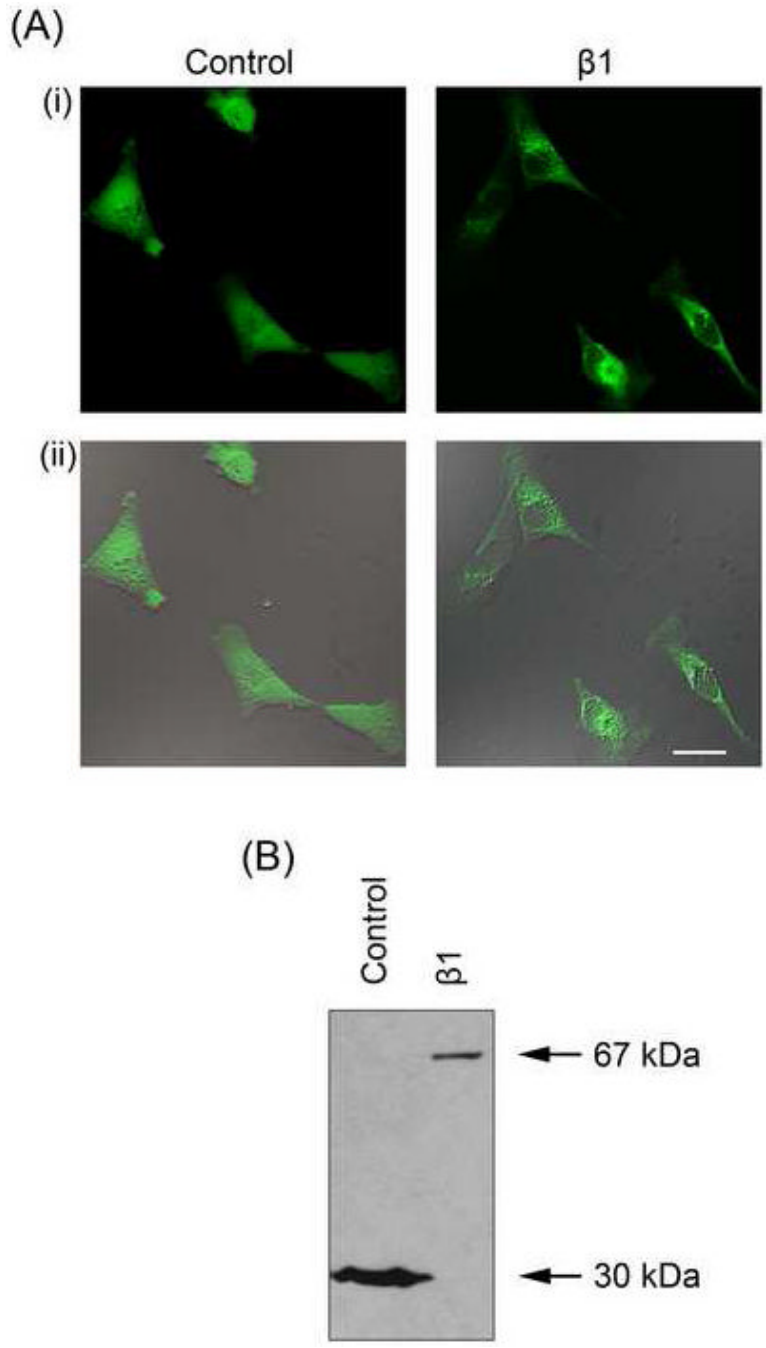

Figure 6. Stably expressing MDA-MB-231 cell lines

(A) Typical confocal XY (i) and merged bright-field images (ii) of MDA-MB-231 cells stably transfected with eGFP ('Control') and β1 with an eGFP C-terminal fusion ('β1'). (B) Western blot of protein from MDA-MB-231 cells stably transfected with eGFP ('Control'; total cell lysate) and β1 with an eGFP C-terminal fusion ('β1'; membrane preparation) using an anti-GFP antibody. eGFP, 30 kDa; β1-eGFP, 67 kDa.

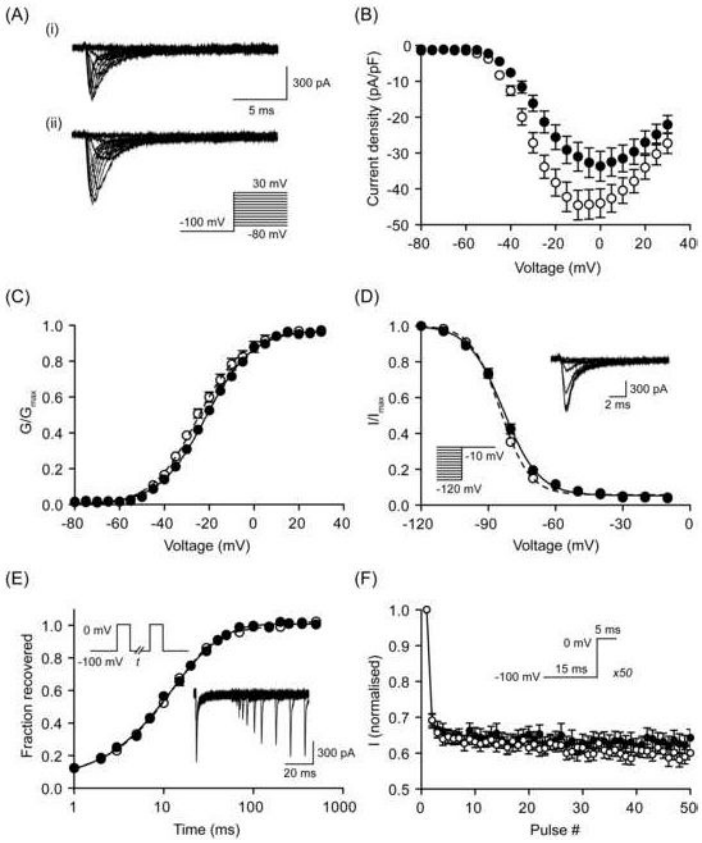

Figure 7. Effect of β1 on VGSC activity in MDA-MB-231 cells

(A) Typical whole-cell Na^+ currents elicited by 60 ms depolarizing voltage pulses between -80 mV and +30 mV applied from a holding potential of -100 mV: (i) a control cell expressing eGFP; (ii) a cell expressing β1-eGFP. (B) Current-voltage relationship. Peak Na^+ current density was plotted as a function of voltage for control cells expressing eGFP (filled circles) and cells expressing β1-eGFP (open circles). (C) Activation. Normalised conductance (G/G_{max}), calculated from the current data, plotted as a function of voltage for control cells expressing eGFP (filled circles) and cells expressing β1-eGFP (open circles). (D) Steady-state inactivation. Normalised current (I/I_{max}), elicited by 60 ms test pulses at - 10 mV following 1 s conditioning voltage pulses between -120 and -10 mV, applied from a holding potential of -100 mV, plotted as a function of the prepulse voltage for control cells expressing eGFP (filled circles) and cells expressing β1-eGFP (open circles). Inset, typical recording from a control cell. (E) Recovery from inactivation. The fraction recovered (I_t/I_0) was determined by a 25 ms pulse to 0 mV (I_0), followed by a recovery pulse to -100 mV for 1-500 ms, and a subsequent 25 ms test pulse to 0 mV (I_t), applied from a holding potential of -100 mV, and plotted as a function of the recovery interval for control cells expressing eGFP (filled circles) and cells expressing β1-eGFP (open circles). Inset, typical recording from a control cell. (F) Use-dependent rundown. Current (I), elicited by 50 Hz pulse trains to 0 mV, applied from a holding potential of-100 mV, normalised to the current evoked by the first pulse plotted as a function of the pulse number for control cells expressing eGFP (filled circles) and cells expressing β1-eGFP (open circles). Control (solid lines) and β1-eGFP (dashed lines) data are fitted with Boltzmann functions, (C) and (D); and double exponential functions, (E). Data are presented as mean ± SEM (n = 20).

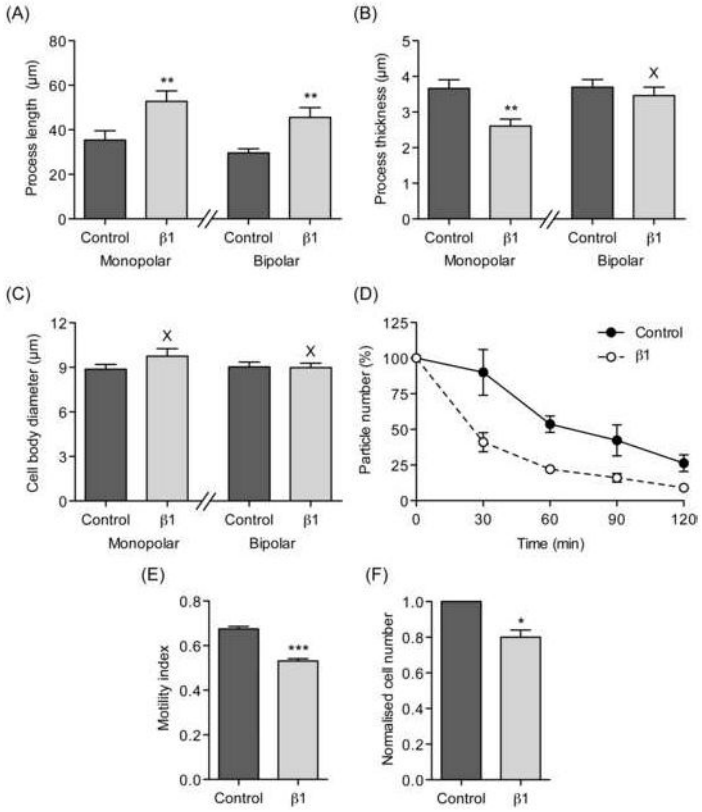

Figure 8. Effects of β1 on morphology, adhesion, migration and proliferation of MDA-MB-231 cells

(A) Process length of MDA-MB-231 cells stably transfected with eGFP ('Control') and β1 with eGFP C-terminal fusion ('β1'). (B) Process thickness of MDA-MB-231 cells stably transfected with eGFP ('Control') and β1 with eGFP C-terminal fusion ('β1'). (C) Cell body diameter of MDA-MB-231 cells stably transfected with eGFP ('Control') and β1 with eGFP C-terminal fusion ('β1'). In (A), (B) and (C), cells were defined as having monopolar or bipolar morphologies and analysed separately (n = 40). (D) Cell-cell adhesion. Single MDA-MB-231 cells stably transfected with eGFP ('Control') and β1 with eGFP C-terminal fusion ('β1') were incubated with gentle agitation for 2 h. The number of particles was monitored every 30 min and expressed as a percentage of the starting value. As cells adhered to one-another and formed aggregates, the particle number decreased (n = 3 repeat experiments). (E) Motility index (MI) of MDA-MB-231 cells stably transfected with eGFP ('Control') and β1 with eGFP C-terminal fusion ('β1') in a wound-heal assay. Wound width was measured at 0 h (W_0) and 24 h (W_t). MI was calculated as $1 - (W_t/W_0)$ (n = 135). (F) Proliferation of MDA-MB-231 cells stably transfected with eGFP ('Control') and β1 with eGFP C-terminal fusion ('β1'), normalised relative to control. Cells were grown for 24 h and counted using the MTT assay (n = 3 repeat experiments). Data are presented as mean ± SEM. Significance: (X) $P > 0.05$; (*) $P < 0.05$, (**) $P < 0.01$, (***) $P < 0.001$; (A), (B), (C), (E) Student's t-test; (F) Student's paired t-test.

Table 1

VGSC β subunit mRNA expression in MCF-7 and MDA-MB-231 human breast cancer cell lines.

A. Fold differences in expression compared between cell lines		
β subunit mRNA	**Fold difference (MCF-7 vs. MDA-MB-231)**	**P**
SCN1B	40	< 0.001
SCN2B	20	< 0.01
SCN4B	50	< 0.001

B. Fold differences within given cell lines			
Cell line	***SCN1B* ≫ *SCN2B***	***SCN4B* > *SCN2B***	***SCN1B* ≫ *SCN4B***
MCF-7	1500-fold	4-fold	450-fold
MDA-MB-231	800-fold	2-fold	500-fold

Table 2

Effect of β1 overexpression on Na^+ current characteristics in MDA-MB-231 cells

Parameter[a]	Control	β1
C_m (pF)	22.4 ± 1.8	19.8 ± 0.9
I_p (pA/pF)	-34.5 ± 4.2	-46.4 ± 4.1 *
I_{per} at -35 mV (pA/pF)	-1.6 ± 0.4	-2.2 ± 0.3
V_a (mV)	-54.0 ± 0.8	-54.5 ± 0.9
V_p (mV)	-1.0 ± 1.2	-4.5 ± 1.5
Activation $V_{1/2}$ (mV)	-21.3 ± 0.9	-23.3 ± 2.6
Activation k (mV)	10.2 ± 0.5	10.0 ± 0.7
Inactivation $V_{1/2}$ (mV)	-83.6 ± 0.8	-84.8 ± 0.6
Inactivation k (mV)	-7.9 ± 0.8	-6.5 ± 0.3
T_p at 0 mV (ms)	0.73 ± 0.03	0.65 ± 0.02 *
τ_f at 0 mV (ms)	0.51 ± 0.03	0.50 ± 0.03
τ_s at 0 mV (ms)	3.7 ± 0.4	3.7 ± 0.4

[a] Abbreviations: C_m, membrane capacitance; I_p, peak current density; I_{per}, persistent current density; V_a, activation voltage; V_p voltage at current peak; $V_{1/2}$, half (in)activation voltage; k, slope factor; T_p time to peak; $\tau_{f/s}$, fast/slow time constant of inactivation.

Data are expressed as mean ± SEM.

* Significance: $P < 0.05$ ($n = 20$).